Suplemento de la Revista Mexicana de Física **3** 0308126 (2022) 1–7

# Holographic model in anisotropic hot dense QGP with external Magnetic Field

K. A. Rannu
*Peoples Friendship University of Russia, Miklukho-Maklaya str.6, 117198, Moscow, Russia*
I. Ya. Aref'eva
*Steklov Mathematical Institute, Russian Academy of Sciences, Gubkina str. 8, 119991, Moscow, Russia*
P. S. Slepov
*Steklov Mathematical Institute, Russian Academy of Sciences, Gubkina str. 8, 119991, Moscow, Russia*

Received 15 January 2022; accepted 17 March 2022

We study the confinement/deconfinement phase diagram within a five-dimensional fully anisotropic holographic model supported by Einstein-dilaton-three-Maxwell action. One of the Maxwell fields provides the chemical potential, the second Maxwell field represents real spacial anisotropy of the QGP produced in heavy-ion collisions and the third Maxwell field is related to an external magnetic field. Influence of the so-called primary anisotropy due to the non-centrality of the heavy-ion collision and secondary anisotropy originating from the external magnetic field on the phase diagram is considered. Based on recent work [1,2].

*Keywords:* AdS/QCD; holography; phase transition; heavy quarks; magnetic field.

DOI: https://doi.org/10.31349/SuplRevMexFis.3.0308126

## 1. Model

The main goal of holographic the QCD is to describe QCD phase diagram, reproducing the results from perturbative theory at short distances, and Lattice results at large distances ($\sim$ 1 fm) and small $\mu_B$ [3–5]. The phase diagram depends on quark mass (Fig. 1a), b)) [6, 7].

In our work we take into account anisotropy to reproduce energy dependence of the total multiplicity of particles created in heavy-ion collisions $\mathcal{M}(s) \sim s^{0.155(4)}$ [8]. Introducing the the anisotropy parameter $\nu$ as $\mathcal{M}(s) \sim s^{1/(\nu+2)}$ leads to the value $\nu \approx 4.5$ for the agreement with the experimental multiplicity data [9].

This kind of anisotropy (let us mark it as primary anisotropy) was systematically studied in previous works [10–16]. This time we add another type of anisotropy, caused by a magnetic field, into consideration (Fig. 1a)). Our reseacrh is also oriented to the future experiments on heavy-ion collisions at high values of baryon density such as NICA project first of all. Therefore, we cannot limit our consideration with zero or small chemical values. As it is well known, standard perturbative methods cannot be applied in this case. Holographic duality method and potential reconstruction are the most promising here.

To describe all the effects we are interested in we take the Lagrangian and the metric ansatz in the following form [1]:

$$\mathcal{L} = R - \frac{f_1(\phi)}{4} F_{(1)}^2 - \frac{f_2(\phi)}{4} F_{(2)}^2 - \frac{f_B(\phi)}{4} F_{(B)}^2 - \frac{1}{2} \partial_\mu \phi \partial^\mu \phi - V(\phi), \tag{1}$$

$$ds^2 = \frac{L^2}{z^2} \mathfrak{b}(z) \left[ - g(z)\, dt^2 + dx^2 + \left(\frac{z}{L}\right)^{2-\frac{2}{\nu}} dy_1^2 + e^{c_B z^2} \left(\frac{z}{L}\right)^{2-\frac{2}{\nu}} dy_2^2 + \frac{dz^2}{g(z)} \right], \tag{2}$$

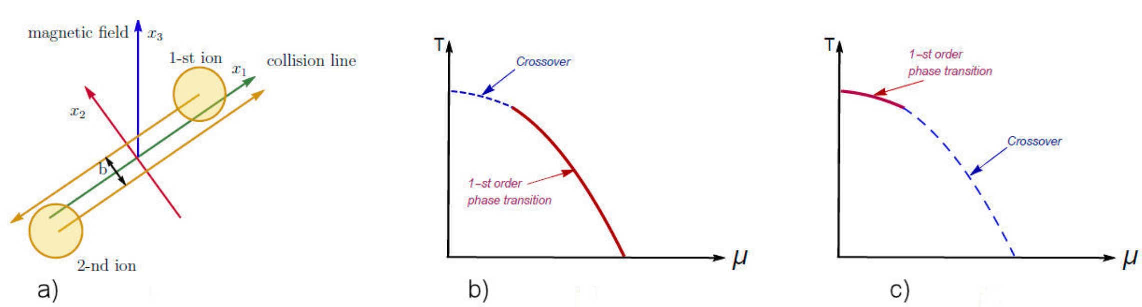

FIGURE 1. Scheme of peripheral HIC a). Qualitative holographic QCD phase diagrams for light b) and heavy c) quarks.

and use the so called "bottom-up appoach" [17-58]. Here $F_{\mu\nu}^{(1)}$, $F_{\mu\nu}^{(2)}$ and $F_{\mu\nu}^{(B)}$ are the Maxwell tensors providing chemical potential, primary anisotropy and magnetic field correspondingly,

$$\begin{aligned} &A_\mu^{(1)} = A_t(z)\delta_\mu^0, \qquad A_t(0) = \mu,\ A_t(z_h) = 0, \\ &F_{\mu\nu}^{(2)} = q\ dy^1 \wedge dy^2, \qquad F_{\mu\nu}^{(B)} = q_B\ dx \wedge dy^1, \end{aligned} \tag{3}$$

whose coupling is set by gauge kinetic functions $f_1(\phi)$, $f_2(\phi)$ and $f_B(\phi)$; $\phi$ and $V(\phi)$ are the scalar field (dilaton) and its potential. The boundary condition for the blackening function $g(z)$ is standard, and the scalar field boundary condition has a significant influence of the string tension $\sigma_{\text{string}}(T)$ [15, 16],

$$g(0) = 1,\ g(z_h) = 0, \quad \phi(z_0) = 0. \tag{4}$$

As it was already noted, quark mass defines the phase diagrams structure. Schematic phase diagram for light and heavy quarks are presented in Fig. 1b) and c). The main difference is in the mutual arrangement of the 1-st order phase transition and a so called crossover. However, we do not introduce the real massive term into the Lagrangian (1), but effectively reproduce these phase diagrams characteristic for heavy or light quarks. For this purpose the form of the warp-factor $\mathfrak{b}(z) = e^{2\mathcal{A}(z)}$ is used, *i.e.* $\mathcal{A}(z) = -cz^2/4$ for the in heavy quarks case (b, t) [17] and $\mathcal{A}(z) = -a\ln(bz^2+1)$ for light quarks case (d, u) [55]. In this work we are interested in the heavy quarks particular case.

Like $\nu \in [1; 4.5]$ determines primary anisotropy, the coefficient $c_B$ paramterizes secondary anisotropy due to the magnetic field. Here and below we assume $L = q_B = 1$ and $c = 0.227$.

Deriving the EOM from the Lagragian (1) with the metric ansatz (2) and solving them, we get the result:

$$A_t = \mu\,\frac{e^{(c-2c_B)z^2/4} - e^{(c-2c_B)z_h^2/4}}{1 - e^{(c-2c_B)z_h^2/4}},\ \rho = -\,\frac{\mu\,(c-2c_B)}{4\left(1 - e^{(c-2c_B)z_h^2/4}\right)},\ f_B = -\,\frac{2c_B\,z^{1-\nu/2}\,g}{q_B^2\,e^{cz^2/2}}\left(\frac{3cz}{2} + \frac{2}{\nu z} - c_B z - \frac{g'}{g}\right), \tag{5}$$

$$\begin{aligned} g = \ e^{c_B z^2}\Bigg\{1 &- \frac{\Gamma\left(1+\frac{1}{\nu}\right) - \Gamma\left(1+\frac{1}{\nu}\,;\frac{3}{4}(2c_B-c)z^2\right)}{\Gamma\left(1+\frac{1}{\nu}\right) - \Gamma\left(1+\frac{1}{\nu}\,;\frac{3}{4}(2c_B-c)z_h^2\right)} - \frac{\mu^2\left(\Gamma\left(1+\frac{1}{\nu}\right) - \Gamma\left(1+\frac{1}{\nu}\,;\frac{3}{4}\,(2c_B-c)\,z^2\right)\right)}{4\,(2c_B-c)^{1/\nu}\left(1 - e^{(c-2c_B)\frac{z_h^2}{4}}\right)^2} \\ &\times\left[1 - \frac{\Gamma\left(1+\frac{1}{\nu}\right) - \Gamma\left(1+\frac{1}{\nu}\,;\frac{3}{4}\,(2c_B-c)z^2\right)}{\Gamma\left(1+\frac{1}{\nu}\right) - \Gamma\left(1+\frac{1}{\nu}\,;\frac{3}{4}\,(2c_B-c)z_h^2\right)}\,\frac{\Gamma\left(1+\frac{1}{\nu}\right) - \Gamma\left(1+\frac{1}{\nu}\,;(2c_B-c)z_h^2\right)}{\Gamma\left(1+\frac{1}{\nu}\right) - \Gamma\left(1+\frac{1}{\nu}\,;(2c_B-c)z^2\right)}\right]\Bigg\}, \end{aligned} \tag{6}$$

$$\phi = \int_{z_0}^{z} \frac{1}{\nu\xi}\sqrt{4\nu - 4 + (4\nu c_B + 3(3c-2c_B)\nu^2)\,\xi^2 + \left(\frac{3}{2}\,\nu^2c^2 - 2c_B^2\right)\xi^4}\ d\xi, \qquad z_0 \neq 0. \tag{7}$$

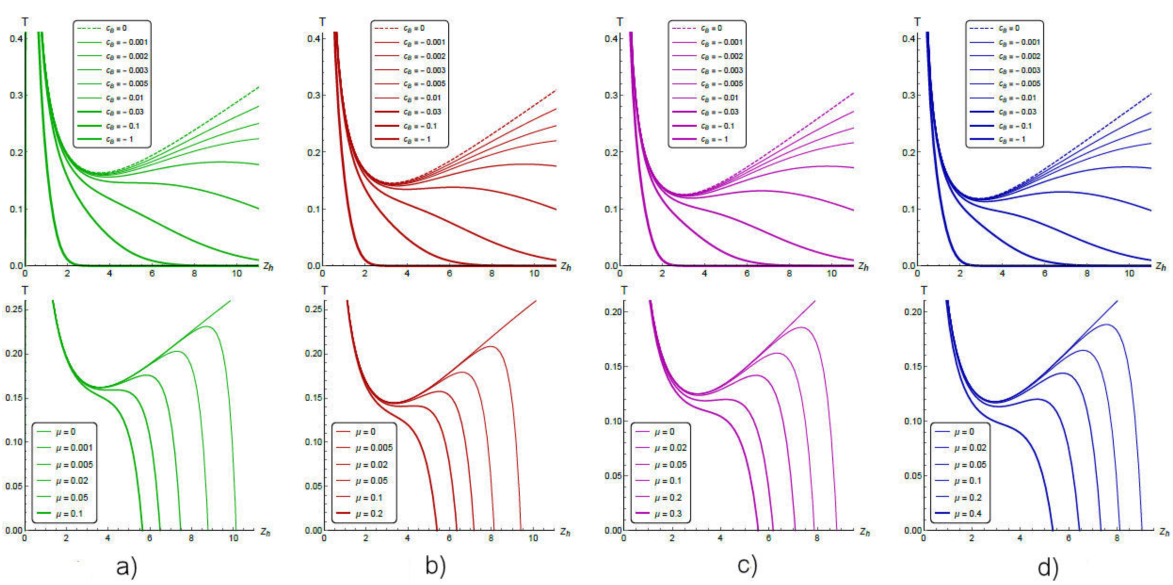


FIGURE 2. Temperature $T(z_h)$ for different $c_B$, $\mu = 0$ (1-st line) and for different $\mu$, $c_B = -0.001$ (2-nd line); $\nu = 1$ a), $\nu = 1.5$ b), $\nu = 3$ c) and $\nu = 4.5$ d), $c = 0.227$.

More detailed discussion of the obtained solution can be found in [1]. Let us note only that the $f_B$-behavior requires $c_B \leq 0$, otherwise NEC is broken.

## 2. Phase diagram

The multivalued behavior of the temperature function $T(z_h)$ makes the collapse from small to large black holes possible. This collapse is interpreted as 1-st order (Hawking-Page-like or background) phase transition within the holographic dictionary (AdS/CFT-correspondence). In Fig. 2 temperature behavior for various magnetic fields and chemical potentials is presented. To be more precise, we do not actually input magnetic field strength or flux density into the EOM, but deal with the result of the magnetic field's impact on the metric, that is expressed by the $c_B$-parameter. We see that for larger metric deformation due to the external magnetic field (larger absolute $c_B$ values) the temperature function's minimum becomes smoother and occasionally disappears (Fig. 2, 1-st line). If $T(z_h)$ is monotonous, no collapse and therefore no background phase transition is possible. An increase in chemical potential has the same effect on temperature (Fig. 2, 2-nd line) like it was in the absence of magnetic field [10]. Both $c_{B\,crit}$ and $\mu_{crit}$, for which the multivalued behavior of $T(x_h)$ is replaced by a monotonous one, depend on primary anisotropy $\nu$. The more anisotropic media is, the greater absolute values of $c_B$ and $\mu$ should be avaliable in phase diagram.

Usual free energy investigation allows to obtain the 1-st order phase transition curves (Fig. 3a)) and verify the reasoning above. A larger magnetic field (*i.e.* larger $c_B$ absolute value) shortens the 1-st order (black hole-black hole or BB) phase transition curves and lowers its temperature. Thus we observe suppression of the phase transition by the magnetic field and the inverse magnetic catalysis. Primary anisotropy ($\nu > 1$) prevents this suppression, but lowers the phase transition temperature even more.

To obtain the full picture we conisder temporal Wilson loops, defined by the following equations:

$$-cz + \sqrt{\frac{2}{3}}\,\phi'(z) + \frac{g'}{2g} - \frac{2}{z}\Big|_{z=z_{DWx}} = 0, \qquad (8)$$

$$-cz + \sqrt{\frac{2}{3}}\,\phi'(z) + \frac{g'}{2g} - \frac{\nu+1}{\nu z}\Big|_{z=z_{DWy_1}} = 0, \qquad (9)$$

$$-cz + \sqrt{\frac{2}{3}}\phi'(z) + \frac{g'}{2g} - \frac{\nu+1}{\nu z} + c_B z\Big|_{z=z_{DWy_2}} = 0. \qquad (10)$$

Generally saying, the magnetic field affects the Wilson loop transition line the same way, *i.e.* lowers temperature, decreases the chemical potential interval and shrinks the phase transition curve. But it is mutual arrangement of the 1-st order and the Wilson loop curves that we are interested in.

In the primary anisotropic case with small magnetic field we have 1-st order phase transition, switching to the crossover (defined by Wislon loop line) for $\mu \geq \mu_{by_2}$ (Fig. 3b)). But the crossover temperature decreases faster than for the 1-st order transition, that finally gets above the crossover and plays no role in the confinement/deconfinement process any more (Fig. 3d)).

In the most anisotropic case with $\nu = 4.5$ the 1-st order phase transition replaces the crossover, defined by the Wilson loop, at some non-zero chemical potential $\mu_{y_2b}$ and lasts until the end $CEP_{HQ}$, where phase transition returns to the crossover with the jump (Fig. 3c)). Such a behavior was discussed in detail in previous works [10, 11]. If the magnetic field grows, the Wilson loop curve shrinks slower than the 1-st order phase transition, whose influence rises, starting from smaller chemical potential. Occasionally all the 1-st transition line gets under the crossover and determines the confinement/deconfinement for all chemical potentials at which it does exist (Fig. 3e)).

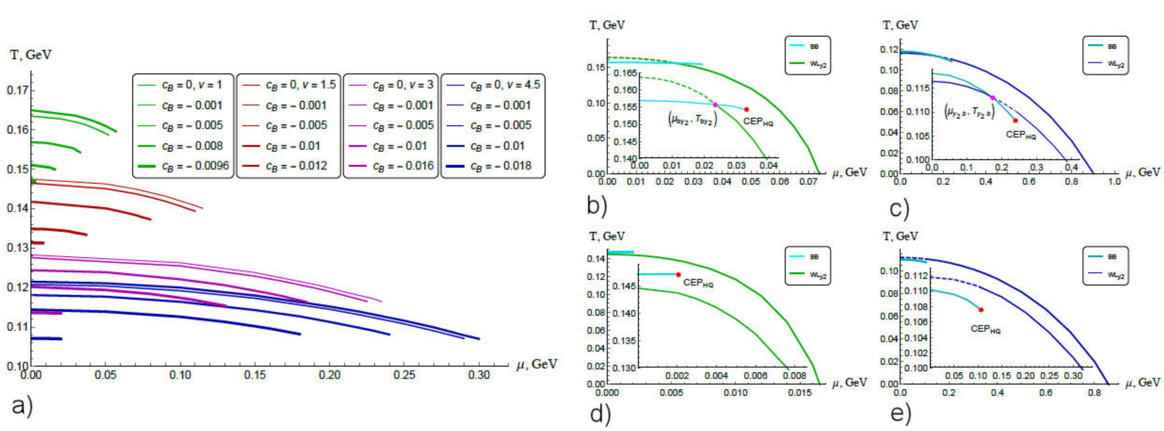


FIGURE 3. 1-st order (BB) phase transitions $T(\mu)$ for different anisotropy $\nu$ and magnetic field $c_B$ a). Phase diagrams for $y_2$-orientation, *i.e.* mutual arrangement of 1-st order phase transition (cyan lines) and Wilson loops (green/blue lines) for $\nu = 1$ b), d) and $\nu = 4.5$ c), e) in magnetic field with $c_B = -0.005$ b), c), $c_B = -0.0096$ d) and $c_B = -0.015$ e). Solid lines mark actual phase diagram curves and dashed lines depict non-realised behavior; $c = 0.227$ and $z_h = 1$.

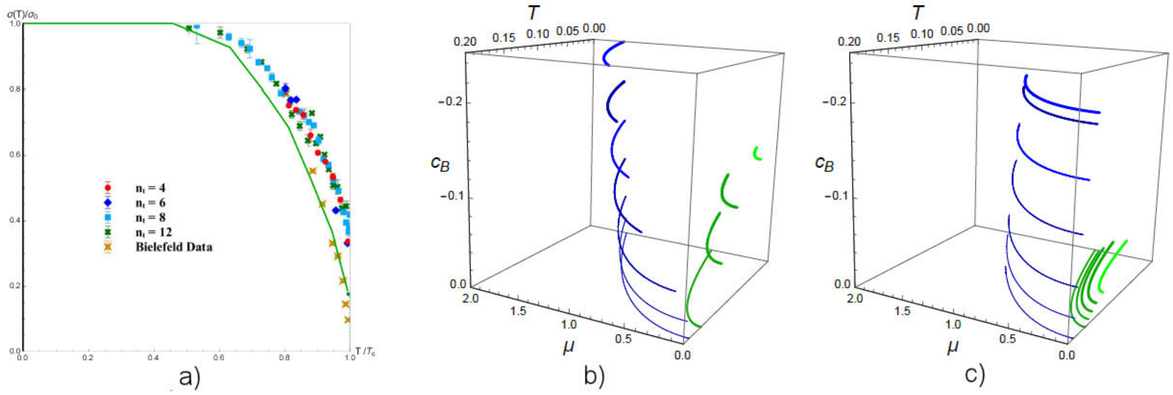


FIGURE 4. Fitting string tension lattice results (dots with different decorations) [59] with $z_0 = 10\exp(-z_h/4) + 0.1$ (green curve), $\mu = 0$, $\nu = 1$ a). Phase transition temperature for the spatial Wilson loops $W_{xY_1}$ b) and $W_{xY_2}$ c) for $\nu = 1$ (green curves) and $\nu = 4.5$ (blue curves) as a function of $\mu$ and $c_B$.

Wilson loops consideration gives a string tension as temperature function. In contrast to the phase transition defined by temporal Wilson loop, string tension does depend on scalar field itself, not on its derivative. Therefore the scalar field boundary condition (4) has an influence on the string tension behavior. Search for proper position $z_0$ allows to fit experimental data or Lattice results [15, 16]. In Fig. 4a) such a fitting of Lattice data [59] for $z_0 = 10\exp(-z_h/4) + 0.1$ is depicted.

Spatial Wilson loops for heavy quarks model in a magnetic field were also considered [2]. It was shown for isotropic models ($\nu = 1$) that the string tension of spatial Wilson loops is proportional to the corresponding drag force [60, 61]. This feature is preserved for anisotropic models [13]. Thus we can estimate energy loss for a quark moving in QGP. Phase transitions between two connected string configurations with different values of string tension $\sigma(z_{DW})$ and $\sigma(z_h)$ are presented in Fig. 4b) and c). This transition means that the dynamic wall disappeared and the string tension can be calculated at horizon only. Phase transition surfaces for primary isotropic ($\nu = 1$) and anisotropic ($\nu = 4.5$) media can be easily imagined as stretched on green or blue curves correspondingly. Light green and blue curves show where the phase transitions stop occuring.

## 3. Conclusions

In this work we obtained a 5D holographic model describing anisotropic hot dense QGP in a magnetic field, and studied the magnetic field influence on the phase diagram, *i.e.* on the interplay between two types of phase transitions: a 1-st order phase transition and a crossover.

We have found the suppression of the 1-st order phase transition by a magnetic field, accompanied by the inverse magnetic catalysis. This effect weakens in cases of primary anisotropy. Though a magnetic field influences the crossover, originating from the Wilson loops, in the same way (crossover undergoes inverse magnetic catalyses as well), the velocity of the temperature fall differs from the 1-st order phase transition and the crossover in primary isotropic and primary anisotropic cases. This leads to the opposite dynamics of the mutual arrangement changes. For $\nu = 1$ the 1-st order phase transition shifts up relative to the crossover and loses any influence on the confinement/deconfinement transition in the strong magnetic field. For $\nu = 4.5$ it on the contrary dives under the crossover and wins a leading role at low chemical potentials and high magnetic field value (Fig. 4b)-e)).

We have also shown that drag forces and therefore energy losses undergo the phase transition depending on anisotropy and magnetic field as well. In spite of the fact that magnetic field's influence on different phase transitions is similar, its effect on the final picture of mutual arrangement "1-st order phase transition/crossover" can be considered as the opposite.

This investigation is just another step in constructing a general holographic picture of confinement/deconfinement process. We have considered an effective description of the heavy quarks case, and the light quarks version is to be done. We have studied phase transitions for the background, temporal and spatial Wilson loops here, but there are some other characteristics such as susceptibility, transport coefficients, direct-photon spectra, jet quenching, thermalization time, etc. These properties should also be discussed both for heavy and light quarks models.

1. I.Ya. Aref'eva, K. Rannu, P. Slepov, *Holographic Anisotropic Model for Heavy Quarks in Anisotropic Hot Dense QGP with External Magnetic Field*, JHEP **07** (2021) 161 https://doi.org/10.1007/JHEP07(2021)161. [arXiv:2011.07023 [hep-th]]
2. I.Ya. Aref'eva, K. Rannu, P. Slepov, *Spatial Wilson loops in a fully anisotropic model*, Theor. Math. Phys. **206** (2021) 349-356 https://doi.org/10.1134/S0040577921030077. [arXiv:2012.05758 [hep-th]]
3. J. Casalderrey-Solana, H. Liu, D. Mateos, K. Rajagopal, U.A. Wiedemann, *Gauge/String Duality, Hot QCD and Heavy Ion Collisions*, (Cambridge University Press, 2014) [arXiv:1101.0618 [hep-th]]
4. I.Ya. Aref'eva, *Holographic approach to quark-gluon plasma in heavy ion collisions*', Phys. Usp. **57** (2014) 527
5. O. DeWolfe, S.S. Gubser, C. Rosen, D. Teaney, *Heavy ions and string theory*, Prog. Part. Nucl. Phys. **75** (2014) 86 [arXiv:1304.7794 [hep-th]]
6. F.R. Brown, F.P. Butler, H. Chen, N.H. Christ, Z. Dong, W. Schaffer, L.I. Unger, A. Vaccarino, *On the existence of a phase transition for QCD with three light quarks*, Phys. Rev. Lett. **65** (1990) 2491-2494 https://doi.org/10.1103/PhysRevLett.65.2491.
7. O. Philipsen, C. Pinke, *The $N_f = 2$ QCD chiral phase transition with Wilson fermions a zero and imaginary chemical potential*, Phys. Rev. D **93** (2016) 114507 https://doi.org/10.1103/PhysRevD.93.114507. [arXiv:1602.06129 [hep-lat]]
8. J. Adam *et al.* [ALICE Collaboration], *Centrality dependence of the charged-particle multiplicity density at midrapidity in Pb-Pb collisions at $\sqrt{s_{\rm NN}} = 5.02$ TeV*, Phys. Rev. Lett. **116** (2016) 222302 https://doi.org/10.1103/PhysRevLett.116.222302. [arXiv:1512.06104 [nucl-ex]]
9. I.Ya. Aref'eva, A.A. Golubtsova, *Shock waves in Lifshitz-like spacetimes*, JHEP **04** (2015) 011 https://doi.org/10.1007/JHEP04(2015)011. [arXiv:1410.4595 [hep-th]]
10. I.Ya. Aref'eva, K.A. Rannu, *Holographic Anisotropic Background with Confinement-Deconfinement Phase Transition*, JHEP **05** (2018) 206 https://doi.org/10.1007/JHEP05(2018)206. [arXiv:1802.05652 [hep-th]]
11. I. Aref'eva, K. Rannu, P. Slepov, *Orientation Dependence of Confinement-Deconfinement Phase Transition in Anisotropic Media'*, Phys. Lett. B **792** (2019) 470-475 https://doi.org/10.1016/j.physletb.2019.04.012. [arXiv:1808.05596 [hep-th]]
12. I. Aref'eva, K. Rannu, P. Slepov, *Cornell potential for anisotropic QGP with non-zero chemical potential*, EPJ Web Conf. **222** (2019) 03023 https://doi.org/10.1051/epjconf/201922203023.
13. I. Aref'eva, *Holography for Nonperturbative Study of QFT*, Phys. Part. Nucl. **51** (2020) 489-496 https://doi.org/10.1134/S1063779620040097.
14. K.A. Rannu, *Holographic Model for Light Quarks in Anisotropic Background*, Phys. Part. Nucl. **52** (2021) 555-559 https://doi.org/10.1134/S1063779621040511.
15. P. Slepov, *A way to improve string tension dependence on temperature in holographic model*, Phys. Part. Nucl. **52** (2021) 560-563 https://doi.org/10.1134/S1063779621040572.
16. I.Ya. Aref'eva, K. Rannu, P. Slepov, *Holographic Anisotropic Model for Light Quarks with Confinement-Deconfinement Phase Transition*, JHEP **06** (2021) 090 https://doi.org/10.1007/JHEP06(2021)090. [arXiv:2009.05562 [hep-th]]
17. O. Andreev, V.I. Zakharov, *On Heavy-Quark Free Energies, Entropies, Polyakov Loop, and AdS/QCD*, JHEP **04** (2007) 100 https://doi.org/10.1088/1126-6708/2007/04/100. [arXiv:hep-ph/0611304 [hep-ph]]
18. U. Gursoy, E. Kiritsis, L. Mazzanti, F. Nitti, *Holography and Thermodynamics of 5D Dilaton-gravity*, JHEP **05** (2009) 033 https://doi.org/10.1088/1126-6708/2009/05/033. [arXiv:0812.0792 [hep-th]]
19. U. Gursoy, E. Kiritsis, L. Mazzanti, F. Nitti, *Improved Holographic Yang-Mills at Finite Temperature: Comparison with Data'*, Nucl. Phys. B **820** (2009) 148-177 https://doi.org/10.1016/j.nuclphysb.2009.05.017. [arXiv:0903.2859 [hep-th]]
20. S. He, M. Huang, Q.-S. Yan, *Logarithmic correction in the deformed $AdS_5$ model to produce the heavy quark potential and QCD beta function*, Phys. Rev. D **83** (2011) 045034 https://doi.org/10.1103/PhysRevD.83.045034. [arXiv:1004.1880 [hep-ph]]
21. M. Mia, K. Dasgupta, C. Gale, S. Jeon, *Heavy Quarkonium Melting in Large N Thermal QCD*, Phys. Lett. B **694** (2011) 460-466 https://doi.org/10.1016/j.physletb.2010.10.023. [arXiv:1006.0055 [hep-th]]
22. U. Gursoy, E. Kiritsis, L. Mazzanti, G. Michalogiorgakis, F. Nitti, *Improved Holographic QCD*, Lect. Notes Phys. **828** (2011) 79-146 https://doi.org/10.1007/978-3-642-04864-7_4. [arXiv:1006.5461 [hep-th]]
23. P. Colangelo, F. Giannuzzi, S. Nicotri, V. Tangorra, *Temperature and quark density effects on the chiral condensate: An AdS/QCD study*, EPJ C **72** (2012) 2096 https://doi.org/10.1140/epjc/s10052-012-2096-9. [arXiv:1112.4402 [hep-ph]]
24. R.-G. Cai, S. He, D. Li, *A hQCD model and its phase diagram in Einstein-Maxwell-Dilaton system*, JHEP **03** (2012) 033 https://doi.org/10.1007/JHEP03(2012)033. [arXiv:1201.0820 [hep-th]]
25. D. Giataganas, *Probing strongly coupled anisotropic plasma*, JHEP **07** (2012) 031 https://doi.org/10.1007/JHEP07(2012)031. [arXiv:1202.4436 [hep-th]]
26. D. Li, M. Huang, Q.-S. Yan, *A dynamical soft-wall holographic QCD model for chiral symmetry breaking and linear confinement*, EPJ C **73** (2013) 2615 https://doi.org/10.1140/epjc/s10052-013-2615-3. [arXiv:1206.2824 [hep-th]]
27. S. He, S.-Y. Wu, Y. Yangm P.-H. Yuan, *Phase Structure in a Dynamical Soft-Wall Holographic QCD Model*, JHEP **04** (2013) 093 https://doi.org/10.1007/JHEP04(2013)093. [arXiv:1301.0385 [hep-th]]

28. D. Li, M. Huang, *Dynamical holographic QCD model for glueball and light meson spectra*, JHEP **11** (2013) 088 https://doi.org/10.1007/JHEP11(2013)088. [arXiv:1303.6929 [hep-ph]]
29. Y. Yang, P.-H. Yuan, *A Refined Holographic QCD Model and QCD Phase Structure*, JHEP **11** (2014) 149 https://doi.org/10.1007/JHEP11(2014)149. [arXiv:1406.1865 [hep-th]]
30. D. Li, S. He, M. Huang, *Temperature dependent transport coefficients in a dynamical holographic QCD model*, JHEP **06** (2015) 046 https://doi.org/10.1007/JHEP06(2015)046. [arXiv:1411.5332 [hep-ph]]
31. R. Rougemont, R. Critelli, J. Noronha, *Holographic calculation of the QCD crossover temperature in a magnetic field*, Phys. Rev. D **93** (2015) 045013 https://doi.org/10.1103/PhysRevD.93.045013. [arXiv:1505.07894 [hep-ph]]
32. Y. Yang, P.-H. Yuan, *Confinement-deconfinement phase transition for heavy quarks in a soft wall holographic QCD model*, JHEP **12** (2015) 161 https://doi.org/10.1007/JHEP12(2015)161. [arXiv:1506.05930 [hep-th]]
33. K. Chelabi, Z. Fang, M. Huang, D. Li, Y.-L. Wu, *Realization of chiral symmetry breaking and restoration in holographic QCD*, Phys. Rev. D **93** (2016) 101901 https://doi.org/10.1103/PhysRevD.93.101901. [arXiv:1511.02721 [hep-ph]]
34. Z. Fang, S. He. D. Li, *Chiral and Deconfining Phase Transitions from Holographic QCD Study*, Nucl. Phys. B **907** (2016) 187-207 https://doi.org/10.1016/j.nuclphysb.2016.04.003. [arXiv:1512.04062 [hep-ph]]
35. K. Chelabi, Z. Fang, M. Huang, D. Li, Y.-L. Wu, *Chiral Phase Transition in the Soft-Wall Model of AdS/QCD*, JHEP **04** (2016) 036 https://doi.org/10.1007/JHEP04(2016)036. [arXiv:1512.06493 [hep-ph]]
36. D. Li, M. Huang, Y. Yang, P.-H. Yuan, *Inverse Magnetic Catalysis in the Soft-Wall Model of AdS/QCD*, JHEP **02** (2017) 030 https://doi.org/10.1007/JHEP02(2017)030. [arXiv:1610.04618 [hep-th]]
37. D. Li, M. Huang, *Chiral phase transition of QCD with $N_f = 2 + 1$ flavors from holography*, JHEP **02** (2017) 042 https://doi.org/10.1007/JHEP02(2017)042. [arXiv:1610.09814 [hep-ph]]
38. D. Dudal, S. Mahapatra, *Confining gauge theories and holographic entanglement entropy with a magnetic field*, JHEP **04** (2017) 031 https://doi.org/10.1007/JHEP04(2017)031. [arXiv:1612.06248 [hep-th]]
39. M.-W. Li, Y. Yang, P.-H. Yuan, *Approaching Confinement Structure for Light Quarks in a Holographic Soft Wall QCD Model*, Phys. Rev. D **96** (2017) 066013 https://doi.org/10.1103/PhysRevD.96.066013. [arXiv:1703.09184 [hep-th]]
40. Y. Yang, P.-H. Yuan, *Universal Behaviors of Speed of Sound from Holography*, Phys. Rev. D **97** (2018) 126009 https://doi.org/10.1103/PhysRevD.97.126009. [arXiv:1705.07587 [hep-th]]
41. I.Ya. Aref'eva, A.A. Golubtsova, G. Policastro, *Exact holographic RG flows and the $A_1 \times A_1$ Toda chain*, JHEP **05** (2019) 117 https://doi.org/10.1007/JHEP05(2019)117. [arXiv:1803.06764 [hep-th]]
42. Z. Fang, Y.-L. Wu, L. Zhang, *Chiral phase transition and QCD phase diagram from AdS/QCD*, Phys. Rev. D **99** (2019) 034028 https://doi.org/10.1103/PhysRevD.99.034028. [arXiv:1810.12525 [hep-ph]]
43. J. Chen, S. He, M. Huang, D. Li, *Critical exponents of finite temperature chiral phase transition in soft-wall AdS/QCD models*, JHEP **12** (2015) 161 [arXiv:1810.07019 [hep-ph]]
44. A.A. Golubtsova, V.H. Nguyen, *Wilson Loops in Exact Holographic RG Flows at Zero and Finite Temperatures*, Theor. Math. Phys. **202** (2020) 214-230 https://doi.org/10.1134/S0040577920020051. [arXiv:1906.12316 [hep-th]]
45. H. Bohra, D. Dudal, A. Hajilou, S. Mahapatra, *Anisotropic string tensions and inversely magnetic catalyzed deconfinement from a dynamical AdS/QCD model*, Phys. Lett. B **801** (2020) 135184 https://doi.org/10.1016/j.physletb.2019.135184. [arXiv:1907.01852 [hep-th]]
46. X. Chen, D. Li, D. Ho, M. Huang, *Quarkyonic phase from quenched dynamical holographic QCD model*, JHEP **03** (2020) 073 https://doi.org/10.1007/JHEP03(2020)073. [arXiv:1908.02000 [hep-ph]]
47. Z. Fang, Y.-L. Wu, *Equation of state and chiral transition in soft-wall AdS/QCD with more realistic gravitational background*, [arXiv:1909.06917 [hep-ph]]
48. Z. Fang, L. Zhang, *Chiral transition and meson melting with finite chemical potential in an improved soft-wall AdS/QCD Model*, [arXiv:1910.02269 [hep-ph]]
49. A. Ballon-Bayona, L.A.H. Mamani, *Nonlinear realization of chiral symmetry breaking in holographic soft wall models*, Phys. Rev. D **102** (2020) 026013 https://doi.org/10.1103/PhysRevD.102.026013. [arXiv:2002.00075 [hep-ph]]
50. S. He, Y. Yang, P.-H. Yuan, *Analytic Study of Magnetic Catalysis in Holographic QCD*, [arXiv:2004.01965 [hep-th]]
51. D. Dudal, A. Hajilou, S. Mahapatra, *A quenched 2-flavour Einstein-Maxwell-dilaton gauge-gravity model*, EPJ A **57** (2021) 142 [arXiv:2103.01185 [hep-th]]
52. A. Ballon-Bayona, J.P. Shock, D. Zoakos, *Magnetic catalysis and the chiral condensate in holographic QCD*, JHEP **10** (2020) 193 [arXiv:2005.00500 [hep-th]]
53. A. Ballon-Bayona, H. Boschi-Filho, E. Folco Capossoli, D.M. Rodrigues, *Criticality from EMD holography at finite temperature and density*, Phys. Rev. D **102** (2020) 126003 [arXiv:2006.08810 [hep-th]]
54. P. Colangelo, F. De Fazio, N. Losacco, *Chaos in a $Q\bar{Q}$ system at finite temperature and baryon density*, Phys. Rev. D **102** (2020) 074016 https://doi.org/10.1103/PhysRevD.102.074016. [arXiv:2007.06980 [hep-ph]]
55. M.-W. Li, Y. Yang, P.-H. Yuan, *Analytic Study on Chiral Phase Transition in Holographic QCD*, JHEP **02** (2021) 055 https://doi.org/10.1007/JHEP02(2021)055. [arXiv:2009.05694 [hep-th]]

56. H. Bohra, D. Dudal, A. Hajilou, S. Mahapatra, *Chiral transition in the probe approximation from an Einstein-Maxwell-dilaton gravity model*, Phys. Rev. D **103** (2021) 086021 [arXiv:2010.04578 [hep-th]]

57. D. M. Rodrigues, D. Li, E. Folco Capossoli, H. Boschi-Filho, *Finite density effects on chiral symmetry breaking in a magnetic field in 2+1 dimensions from holography*, Phys. Rev. D **103** (2021) 066022 [arXiv:2010.06762 [hep-th]]

58. N. Jokela, J.G. Subils, *Is entanglement a probe of confinement?*, JHEP **02** (2021) 147 [arXiv:2010.09392 [hep-th]]

59. N. Cardoso, P. Bicudo, *Lattice QCD computation of the SU(3) String Tension critical curve*, Phys. Rev. D **85** (2012) 077501 `https://doi.org/10.1103/PhysRevD.85.077501`. [arXiv:1111.1317 [hep-lat]]

60. S.J. Sin, I. Zahed, *Ampere's Law and Energy Loss in AdS/CFT Duality*, Phys. Lett. B **648** (2007) 318 `https://doi.org/10.1016/j.physletb.2007.01.074`. [arXiv:0606049 [hep-th]]

61. O. Andreev, *Drag Force on Heavy Quarks and Spatial String Tension*, Mod. Phys. Lett. A **33** (2018) 1850041 `https://doi.org/10.1142/S0217732318500414`. [arXiv: 1707.05045[hep-ph]]